
FUEL PIN PRELIMINARY DESIGN

Nuclear Engineering – Politecnico di Milano

Simone Pagliuca, Tommaso Pirola, Lisa Raffuzzi, Riccardo Ronchi, Darien Shabi

simone1.pagliuca@mail.polimi.it

Course: Nuclear Design and Technologies

Academic year: 2024/2025

ABSTRACT: lorem ipsum dolor sit amet, consectetur adipiscing elit. Donec auctor, nunc nec ultricies ultricies, nunc nunc.

Key-words: Key, Words, Here

CONTENTS

1	Introduction	3
2	Problem Description	3
3	Assumptions	3
4	Verification of Models	4
4.1	Thermal-Hydraulics Analysis	4
4.2	Temperature Profiles	5
4.3	Thermal Expansion	6
4.4	Void Swelling	7
4.5	Fission Gas Behavior	8
4.6	Restructuring	9
4.7	Stress Analysis	10
4.8	Helium Embrittlement	10
5	Plenum Design	11
6	Plenum Design	12
7	Future Work	12
A	Code Listings	12

1 INTRODUCTION

This report presents the preliminary design and verification of a fuel pin for a sodium-cooled fast reactor, as specified in the assignment.

The analysis involves calculations for material properties, thermal-hydraulic conditions, and mechanical stress limits.

We verify the robustness of our models and justify the assumptions made throughout the process.

2 PROBLEM DESCRIPTION

The fuel pin design problem requires:

- Determining the cladding thickness, fuel-cladding gap size, and plenum height.
- Verifying the design against limits for fuel melting, cladding temperature, yielding, and rupture time.
- Identifying critical aspects if irradiation time is doubled.

The project specifications and material properties are summarized in Table 1.

Table 1: Fuel pin design specifications.

PLACEHOLDER
IMAGE
TO BE
REPLACED

3 ASSUMPTIONS

To address the given problem, the following assumptions were made:

Steady State Solution for Gas in Grains:

- ↔ The rate equation for the gas remaining in the grains (PDE) was solved in steady state conditions, given that we just want to size the plenum for 1-year operation and are not interested in the specific behavior in time of the function.

Fission Rate Calculation:

- ↔ The fission rate was calculated by using the formula (macroscopic cross section * average flux).
- ↔ The macroscopic cross section of fission was computed from data taken from the JANIS database.
- ↔ The average flux was evaluated considering power and flux profile to be equal.

Material Properties and Geometry:

- ↔ Material properties are temperature-dependent and were modeled using provided empirical correlations.
- ↔ Axial power and neutron flux profiles remain constant over time.
- ↔ Initial helium pressure and temperature in the fuel-cladding gap were assumed as specified.
- ↔ Simplifications in geometry, such as neglecting axial deformation, were made to ease computation.

4 VERIFICATION OF MODELS

Each function used in the analysis was tested for expected behavior.

Below are the key verification steps.

4.1 Thermal-Hydraulics Analysis

Preliminary checks were conducted on coolant properties.

Density, viscosity, and thermal conductivity were validated at the coolant inlet temperature.

The heat transfer coefficient between the coolant and cladding was computed using Nusselt number correlations.

Figure 1 shows the axial power profile. the computed heat transfer coefficient in cold geometry was $\alpha_{coolant} = 139.98 \frac{kW}{m^2K}$.

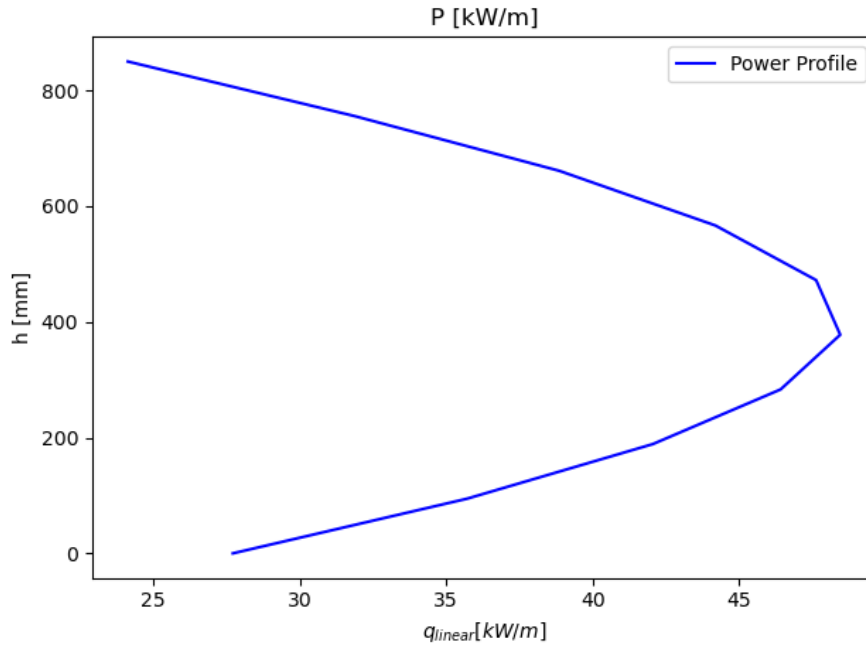


Figure 1: Thermal-hydraulics analysis results.

4.2 Temperature Profiles

Radial and axial temperature profiles were computed for the cold geometry to check if the shape of the profile made sense and if the values were reasonable.

We create a temperature map of the fuel rod. For every node along the axial direction, we first compute the temperature increase in the coolant due to the heat generated in the fuel. From this we compute the temperature at the coolant cladding interface using the heat transfer coefficient (computed by given correlations). For the cladding again we approximate to a linear temperature profile and compute the temperature at the cladding gas interface. Then for the gap and the fuel we compute several temperature points along the radius, at every step the properties are updated to the temperature of the previous step. The inner void is at the same temperature as the inner surface of the fuel.

The results provided an initial validation of the temperature distribution behavior before further analysis.

Figure 2 illustrates the temperature along the axis, at the interfaces, while Figure 3 shows the radial temperature profiles at the bottom, middle and top of the fuel rod.

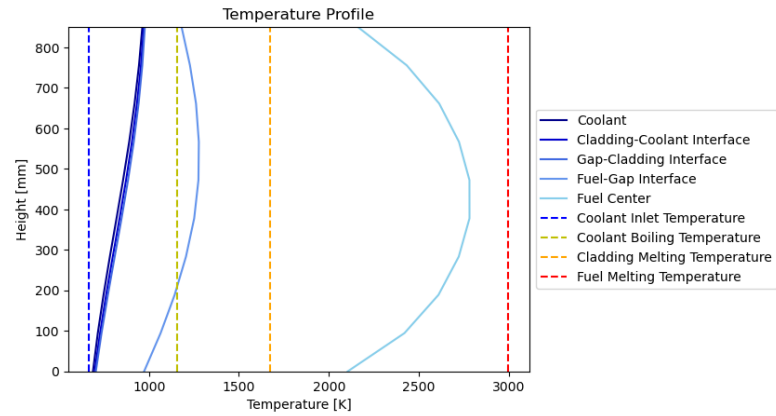


Figure 2: Axial temperature profile for cold geometry.

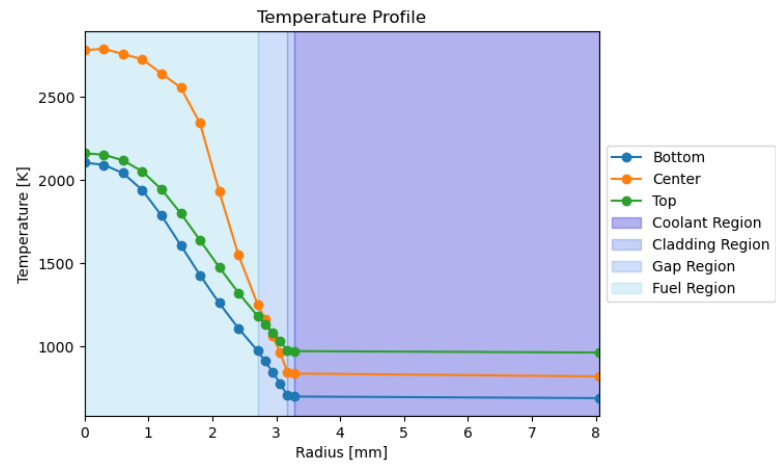


Figure 3: Radial temperature profile for cold geometry.

4.3 Thermal Expansion

Figure 4 shows



Figure 4: Cladding swelling due to void formation.

4.4 Void Swelling

A correlation for the volumetric void swelling of the cladding was given. We assumed the swelling to be isotropic and therefore the radial expansion is $\frac{1}{3}$ of the volumetric expansion. Figure 5 shows the swelling of the cladding along the axial direction. We can see that, as expected, the swelling is only contained within a range of temperature: too low and no swelling, too high and the mobility is high enough that recombination prevails.

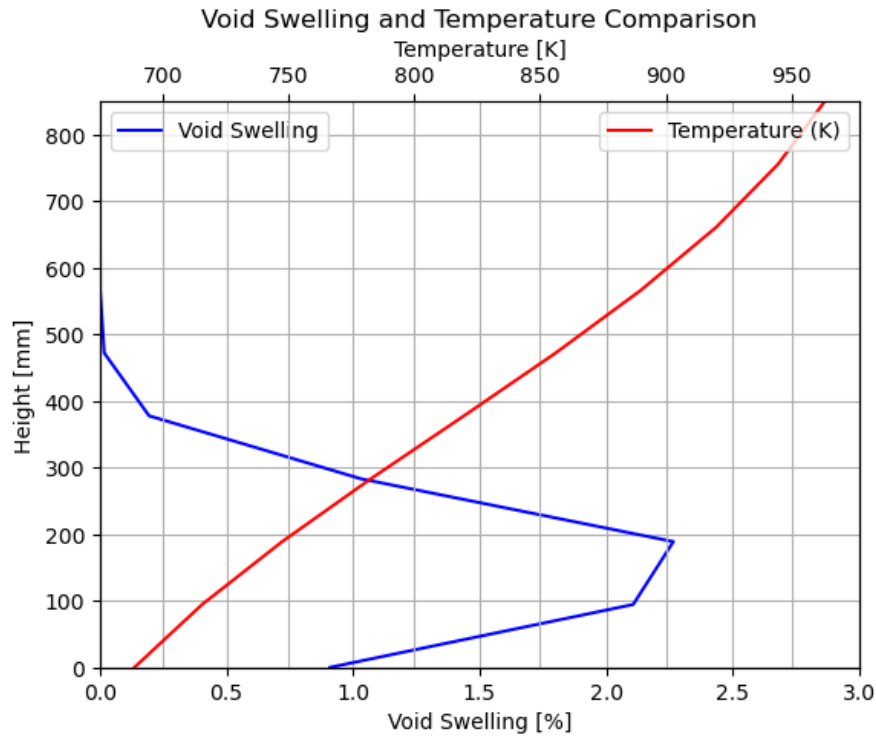


Figure 5: Cladding swelling due to void formation.

4.5 Fission Gas Behavior

Rate theory equations were solved to estimate fission gas production and release over the fuel cycle.

The rate equation for the gas remaining in the grains was solved under steady state conditions, given that we are only interested in sizing the plenum for 1-year operation.

The fission rate was calculated as the product of the macroscopic cross section and the average flux.

The macroscopic cross section was obtained from data in the JANIS database, and the average flux was estimated by assuming the power and flux profiles were equivalent.

The concentration profiles are shown in Figure 6.



Figure 6: Fission gas concentration profiles.

4.6 Restructuring

After transitioning from cold geometry to hot geometry and evaluating the thermal expansion we have to take in account the fuel restructuring process. We make some assumption about columnar and equiaxed region-radii, as well as on densities in different regions. We set the temperature boundaries for columnar region at 1800°C and at 1600°C for equiaxed region, according to Holander's book. Regarding the densities, we consider that in the As-fabricated region the density remains the same, while in the equiaxed a percentage of TD of 95. First of all, we evaluate columnar and equiaxed radii respectively at 1800°C and 1600°C as we said, based on a temperature map. This map provides the temperature at different heights along the fuel pin, using a precise function that allows us to determine the temperature at any position in the 3D model previously developed. Once columnar and equiaxed radii are determined, we have to evaluate the void radius. The As-fabricated region is only the remaining portion of the fuel outer radius after subtracting the equiaxed region. Using this simple correlation to make a possible solution of void formation:

$$R_{void} = \sqrt{R_{col}^2 - R_{eq}^2 \cdot \left(\frac{\text{Density}_{AS}}{\text{Density}_{col}} \right) + (R_{eq}^2 - R_{col}^2) \cdot \left(\frac{\text{Density}_{eq}}{\text{Density}_{AS}} \right)} \quad (1)$$

At end, there is the plot of the fuel element: height vs Radius. We want to show the restructuring phenomenon and highlight the contributions' dependence on the axial position-z of the fuel pin. Figure 7 shows

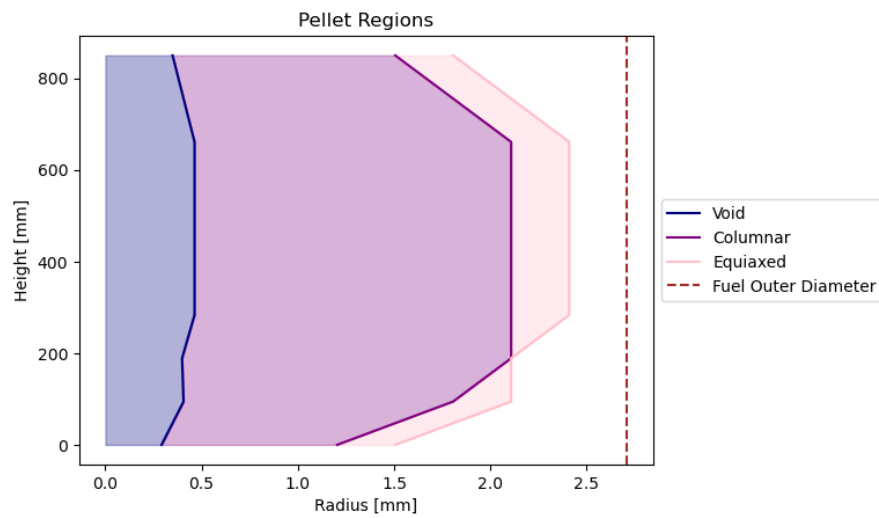


Figure 7: Cladding swelling due to void formation.

4.7 Stress Analysis

Figure 8 shows



Figure 8: Cladding swelling due to void formation.

4.8 Helium Embrittlement

Figure 9 shows the swelling of the cladding along the axial direction.



Figure 9: Cladding swelling due to void formation.

5 PLENUM DESIGN

The relationship between plenum height and pressure was analyzed to ensure the pressure remains below 5 MPa.

Figure 10 shows the results.



Figure 10: Plenum pressure as a function of height.

6 PLENUM DESIGN

The relationship between plenum height and pressure was analyzed to ensure the pressure remains below 5 MPa.

Figure 11 shows the results.



Figure 11: Plenum pressure as a function of height.

7 FUTURE WORK

In subsequent steps, we will develop a dimensioning loop to automate the iterative design process.

We will present final results, including optimized dimensions and safety margins, and comment on the design's robustness under extended irradiation.

A CODE LISTINGS

Placeholder for code files.